RSC Advances

PAPER

View Article Online
View Journal | View Issue

Cite this: *RSC Adv.*, 2026, **16**, 14027

Synthesis and *in vitro* antitumor evaluation of novel 3,4-dihydropyrimidinone-vorinostat hybrids against gastric and breast cancer cell lines

E. A. M. Rios,[a] G. M. S. D. M. Pereira,[b] M. G. M. D'Oca,[b] C. M. Dea,[a] E. R. F. B. Santos,[a] D. S. Rampon,[a] L. S. Santos,[c] F. M. Nachtigall,[c] L. Guzman,[c] R. Moore-Carrasco,[c] D. Rebolledo-Miraf[c] and C. R. M. D'Oca *[a]

Novel 5-substituted dihydropyrimidinones (DHPMs) bearing a methoxy terminal group, together with DHPM–SAHA molecular hybrids inspired by the clinically approved antitumour agent Vorinostat (SAHA), were synthesised *via* the Biginelli multicomponent reaction and evaluated for their *in vitro* antitumour activity against AGS (gastric) and MCF-7 (breast) cancer cell lines. All compounds exhibited low cytotoxicity towards human fibroblasts (SW872), maintaining cell viabilities ≥70%. The derivatives displayed pronounced antiproliferative activity, particularly against MCF-7 cells, consistently showing higher potency than when against AGS cells and, in several cases, superior activity compared to Monastrol. Within the ester DHPM series, three compounds exhibited IC_{50} values below 5 μM, with derivative **6a** emerging as the most active ester analogue ($IC_{50} = 1.33 \pm 0.09$ μM). Notably, substitution of the terminal ester by a hydroxamic acid moiety—responsible for Zn^{2+} chelation in HDAC inhibition and central to Vorinostat's antitumour mechanism—resulted in a marked enhancement of antiproliferative activity, yielding highly potent DHPM–SAHA hybrids. Several hybrids displayed submicromolar IC_{50} values against MCF-7 cells, irrespective of the aromatic substituent, with four compounds exhibiting IC_{50} values below 1 μM and a further four below 5 μM. Among them, DHPM–SAHA hybrid **7i**, derived from 4-methoxybenzaldehyde, emerged as the most potent compound ($IC_{50} = 0.02 \pm 0.00$ μM). Collectively, these results underscore the successful integration of DHPM and HDAC-inhibitory pharmacophores and highlight DHPM–SAHA hybrids as promising multitarget scaffolds for the development of new breast cancer therapeutics.

Received 26th January 2026
Accepted 3rd March 2026

DOI: 10.1039/d6ra00701e

rsc.li/rsc-advances

Introduction

The search for innovative drug discovery strategies has intensified due to the high costs, extended timelines and low success rates associated with conventional drug development. Traditional approaches typically require 10–15 years of research and exhibit an overall success rate of approximately 2%.[1] In this context, molecular hybridisation has emerged as a promising strategy for the identification of new biologically active compounds. This approach involves the rational combination of distinct pharmacophoric moieties with known biological activities into a single molecular framework, enabling the design of new chemical entities with enhanced or synergistic pharmacological profiles, multitarget activity and potentially reduced adverse effects.[2]

By integrating compounds with well-established pharmacodynamic and pharmacokinetic properties, molecular hybridisation has driven substantial advances in medicinal chemistry. A broad range of therapeutic targets has been explored using this strategy, particularly in cancer therapy. Importantly, molecular hybrids have also shown promise in overcoming multidrug resistance, a major limitation of conventional chemotherapy in which tumour cells become unresponsive to multiple anticancer agents.[3] Accordingly, hybrid molecules acting as multitarget anticancer agents are regarded as an effective approach to address key challenges in cancer treatment, including therapeutic resistance and the inherent limitations of combination therapies.[4] The translational relevance of this strategy is underscored by the growing number of molecular hybrids currently in clinical trials or already approved for therapeutic use.[5,6]

Among the compound classes exhibiting well-established anticancer activity through the induction of apoptosis are dihydropyrimidinones (DHPMs).[7–9] These heterocyclic scaffolds are readily accessible *via* the Biginelli multicomponent reaction (MCR), first reported by Pietro Biginelli in 1893.[8] This one-pot

[a]*Laboratory of Polymers and Catalysis (LAPOCA), Department of Chemistry, Federal University of Parana – UFPR, P. O. Box 19032, Curitiba, PR, 81531-990, Brazil. E-mail: carolinedoca@ufpr.br*

[b]*Laboratory KOLBE of Organic Synthesis, Department of Chemistry, Federal University of Parana – UFPR, P. O. Box 19032, Curitiba, PR, 81531-990, Brazil*

[c]*Institute of Natural Resources, Universidad de Talca, Talca 3460000, Chile*

condensation of a nitrogen source (*e.g.*, urea or thiourea), an aldehyde and a 1,3-dicarbonyl compound affords DHPMs as a versatile class of N-heterocycles with a wide range of biological and pharmacological applications.[8–11] Notably, Monastrol is one of the most prominent DHPMs and was identified as a selective inhibitor of the mitotic kinesin Eg5. By targeting this motor protein, which is overexpressed in several cancer types including breast, lung, pancreatic, ovarian and bladder cancers, Monastrol disrupts spindle formation, thereby inhibiting cell division and tumour cell proliferation.[12,13]

In contrast, Vorinostat (**1**, Fig. 1)[14] is a nitrogen-containing compound that exerts its antitumour activity through chelation of the Zn^{2+} ion located in the catalytic domain of histone deacetylases (HDACs).[15] This mechanism underlies its ability to modulate epigenetic regulation and selectively target tumour cells.[16] Vorinostat, also known as suberoylanilide hydroxamic acid (SAHA), was approved in 2006 for the treatment of cutaneous T-cell lymphoma and functions as a pan-inhibitor of class I and II HDACs.[17]

Recent studies have highlighted hydroxamic acid–based molecular hybrids as particularly effective HDAC inhibitors. Coumarin-derived hydroxamic acids, for example, have emerged as potent HDACis, combining the coumarin scaffold with zinc-binding hydroxamic acid moieties.[18] These hybrids exhibited enhanced antiproliferative activity against MDA-MB-231 and MCF-7 breast cancer cell lines (IC_{50} = 0.36–2.91 μM) compared with Vorinostat (IC_{50} = 1.33 and 4.15 μM, respectively), while remaining non-toxic toward normal Beas-2B and L-02 cells.[19,20] The phenyl group within the coumarin scaffold enables π–π interactions with tyrosine residues in the HDAC active site, contributing to effective Zn^{2+} chelation by the hydroxamic acid. Ferrocene–hydroxamic acid hybrids have also demonstrated excellent inhibitory activity against HDAC6, with IC_{50} values in the nanomolar range, as well as significant antiproliferative effects against 4T1 breast cancer cells.[21]

Despite their structural diversity, most HDAC inhibitors share a common pharmacophoric architecture that reflects the topology of the HDAC active site. As illustrated in Fig. 1, this pharmacophore comprises three key elements: a surface recognition cap group (CAP) that interacts with amino acid residues at the rim of the active site; a zinc-binding group (ZBG) responsible for chelating the catalytic Zn^{2+} ion; and a linker domain that occupies the hydrophobic channel of the enzyme.[22]

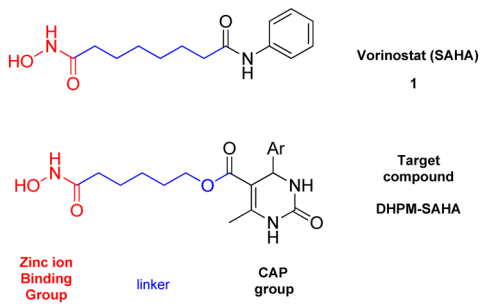

Fig. 1 Structures of Vorinostat/SAHA (**1**), recognized for their antitumor activity, and novel DHPM–SAHA hybrids proposed.

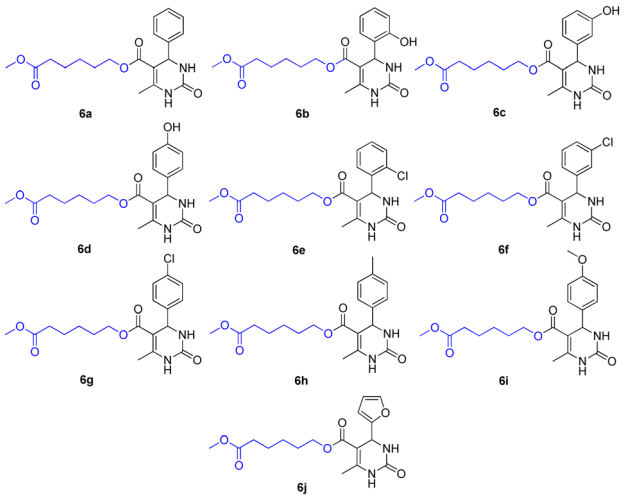

Fig. 2 Structures of 5-substituted DHPMs (**6a–j**) bearing a methoxy terminal group obtained *via* the Biginelli multicomponent reaction.

In this context, and considering the structural diversity of N-heterocycles accessible through the Biginelli multicomponent reaction—together with the reported antitumour performance of monastrol–melatonin hybrids[23] and our previous studies demonstrating the antitumoral potential of Biginelli-derived hybrids[24–27]—this work reports the multistep synthesis and *in vitro* antitumour evaluation of novel DHPM–SAHA molecular hybrids (Fig. 2). These compounds were evaluated against breast (MCF-7) and gastric (AGS) cancer cell lines, aiming to explore the synergistic integration of DHPM and HDAC-inhibitory pharmacophores.

Results and discussion

Initially, β-ketoester **5** was synthesised in two steps. In the first step, ring opening of the seven-membered lactone ε-caprolactone (**2**) was performed in methanol under acidic conditions using sulfamic acid (H_2NSO_3H, SA, 30 mol%) as catalyst. Sulfamic acid is a stable, inexpensive and environmentally benign solid, which has been widely employed as an efficient green catalyst in organic synthesis.[28] After 4 h, the corresponding hydroxyester **3** was obtained in quantitative yield. In the second step, acylation of compound **3** with TMD **4** (2,2,6-trimethyl-4*H*-1,3-dioxin-4-one) was carried out in the presence of anhydrous NaOAc in THF, affording β-ketoester **5** in 62% yield (Scheme 1).

The next step involved a Biginelli multicomponent reaction (MCR) employing the 1,3-dicarbonyl compound **5**, a series of aromatic aldehydes bearing either electron-donating or electron-withdrawing substituents, urea, and sulfamic acid (SA, 20 mol%) as the catalyst. The versatility of SA allows its application in a wide range of acid-catalysed organic reactions.[29]

The reactions were carried out following established literature procedures, affording the 5-substituted DHPMs bearing a methoxy terminal group (**6a–i**, Fig. 3) in yields ranging from 30% to 70%. The resulting products were purified by recrystallisation.

Subsequently, the final step involved the aminolysis of DHPMs **6a–j** with hydroxylamine hydrochloride under basic

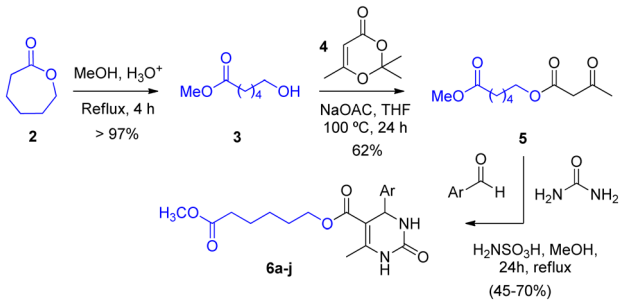

Scheme 1 Synthesis of DHPMs **6a–j** from ε-caprolactone (**2**).

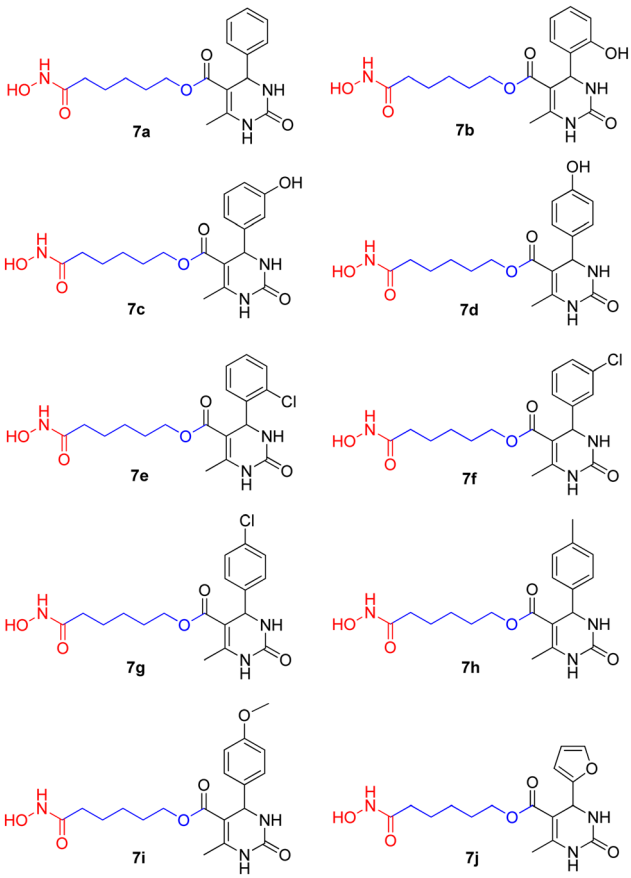

Fig. 3 5-Substituted DHPMs-SAHA molecular hybrids **7a–j**.

conditions (KOH). The reactions were carried out at 25 °C for 24 h, with the pH maintained above 10 (Scheme 2). The resulting hydroxamic acid–containing hybrids, designated as DHPM–SAHA hybrids **7a–j**, were purified by recrystallisation, affording yields in the range of 42–66%. The structures of the hybrids were confirmed by spectroscopic and spectrometric analyses (see SI) and are depicted in Fig. 3.

Both the DHPM–SAHA hybrids **7a–j** and their corresponding methoxylated DHPM precursors **6a–j** were evaluated for *in vitro* antitumour activity against AGS and MCF-7 cell lines, representative of gastric and breast cancers, respectively. Initially, MTT assays were performed to evaluate the effects of the compounds on cell viability using the SW872 cell line, a human

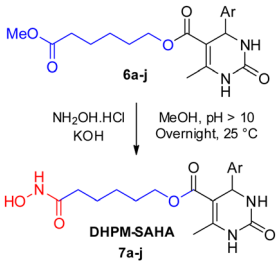

Scheme 2 Synthesis of DHPM–SAHA molecular hybrids **7a–j**.

liposarcoma (malignant) cell model. SW872 has been widely employed in cancer research, particularly for the evaluation of novel anticancer agents, due to its demonstrated sensitivity to several established chemotherapeutic drugs. All experiments were performed in triplicate (Fig. 4).

As shown in Fig. 4, the 5-substituted DHPMs **6a–j** and **7a–j**, bearing methoxy and hydroxamic acid terminal groups, respectively, exhibited cell viabilities close to or above 70% in human fibroblast cells (SW872), indicating low or negligible cytotoxicity and thus being classified as non-cytotoxic. Consequently, all compounds were selected for further evaluation against the AGS (gastric) and MCF-7 (breast) cancer cell lines. The antiproliferative activities are expressed as IC_{50} values (μM) and are summarised in Table 1.

Cells were seeded in 96-well plates at a density of 5000 cells per well and allowed to adhere for 12 h. Subsequently, each DHPM compound was applied at a final concentration of 10 μM and incubated for 48 h. For determination of the half-maximal inhibitory concentration (IC_{50}), the same experimental procedure was followed, using compound concentrations ranging from 0.1 μM to 1000 μM. Monastrol was employed as the reference compound.[24]

Evaluation of the 5-substituted DHPMs **6a–j**, bearing a methoxy terminal group, revealed notable antitumor activity, particularly against the breast cancer cell line (MCF-7). As shown in Table 1 (entries 1–10), all tested DHPMs exhibited significant cytotoxic effects against MCF-7 cells, regardless of

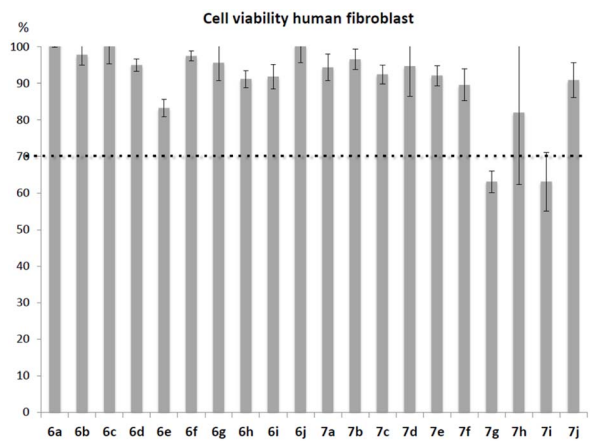

Fig. 4 MTT results of compounds (10 μM) in the viability (%) of human fibroblast cells (SW872).

Table 1 IC_{50} values against cancer cells (AGS and MCF-7), upon application of DHPMs **6a–j** and DHPM–SAHA **7a–j** at 10 μM

	Compound		IC_{50} (μM)	
Entry	Aromatic moeity	Carboxilic group	AGS	MCF-7
1	**6a**, Ph	MeO^-	135.03 ± 20.29	1.33 ± 0.09
2	**6b**, 2-OH-Ph		106.67 ± 4.21	8.79 ± 12.11
3	**6c**, 3-OH-Ph		144.45 ± 21.14	13.83 ± 5.83
4	**6d**, 4-OH-Ph		109.94 ± 14.80	9.65 ± 8.09
5	**6e**, 2-Cl-Ph		71.12 ± 43.85	38.09 ± 12.37
6	**6f**, 3-Cl-Ph		148.13 ± 32.85	87.48 ± 125.10
7	**6g**, 4-Cl-Ph		156.43 ± 6.07	10.36 ± 2.01
8	**6h**, 4-Me-Ph		125.76 ± 43.32	2.33 ± 1.58
9	**6i**, 4-MeO-Ph		120.20 ± 17.45	2.75 ± 0.89
10	**6j**, furanyl		138.17 ± 18.18	40.17 ± 9.50
11	**7a**, Ph	$HO\text{-}NH^-$	64.73 ± 0.48	2.36 ± 0.65
12	**7b**, 2-OH-Ph		22.12 ± 3.30	3.61 ± 0.40
13	**7c**, 3-OH-Ph		14.14 ± 2.50	12.85 ± 4.79
14	**7d**, 4-OH-Ph		165.20 ± 4.08	18.18 ± 6.12
15	**7e**, 2-Cl-Ph		17.02 ± 0.80	3.32 ± 0.57
16	**7f**, 3-Cl-Ph		6.70 ± 2.91	0.52 ± 0.20
17	**7g**, 4-Cl-Ph		5.18 ± 0.89	0.03 ± 0.01
18	**7h**, 4-Me-Ph		10.83 ± 2.68	0.04 ± 0.02
19	**7i**, 4-MeO-Ph		17.12 ± 0.87	0.02 ± 0.00
20	**7j**, furanyl		10.19 ± 1.46	1.21 ± 0.46
21	Monastrol		38.2 ± 3.52	22.5 ± 6.31

the nature of the aromatic substituent, with IC_{50} values ranging from 1.33 ± 0.09 to 87.48 ± 125.10 μM. Overall, these compounds were more active against MCF-7 than against the gastric cancer cell line (AGS) and, in several cases, displayed superior activity compared to Monastrol (IC_{50} = 22.5 ± 6.31 μM against MCF-7; Table 1, entry 21).

In contrast, against AGS cells, DHPMs **6a–j** exhibited substantially higher IC_{50} values than Monastrol (38.2 ± 3.52 μM), indicating low cytotoxic activity, with IC_{50} values ranging from 71.12 ± 43.85 to 156.43 ± 6.07 μM.

Among the evaluated compounds, **6a**, **6h**, and **6i** emerged as the most promising candidates against MCF-7 cells, all exhibiting IC_{50} values below 5 μM. Notably, the ester derivative **6a** (Table 1, entry 1), synthesized from benzaldehyde, displayed the lowest IC_{50} value (1.33 ± 0.09 μM), representing the most potent compound within the ester DHPM series. Additionally, derivatives **6h** and **6i** obtained from 4-methylbenzaldehyde and 4-methoxybenzaldehyde (Table 1, entries 8 and 9) also demonstrated high potency, with IC_{50} values of 2.33 ± 1.58 μM and 2.75 ± 0.89 μM, respectively.

Introduction of a terminal hydroxamic acid group into the side chains (Table 1, entries 11–20), derived from the corresponding ester precursors, resulted in a marked enhancement of *in vitro* antiproliferative activity for the DHPM–SAHA hybrid derivatives **7a–j**.

The IC_{50} values for this series ranged from 0.02 ± 0.00 to 18.18 ± 6.12 μM against MCF-7 breast cancer cells, and from 5.18 ± 0.89 to 165.20 ± 4.08 μM against AGS gastric cancer cells. Similar to the behaviour observed for the 5-substituted DHPMs **6a–j** bearing a methoxy terminal group, the DHPM–SAHA hybrids **7a–j** proved to be particularly promising against MCF-7 cells, with all derivatives displaying substantially lower IC_{50} values than Monastrol (22.5 ± 6.31 μM; Table 1, entry 21).

Against AGS cells, eight compounds (**7b**, **7c** and **7e–j**) bearing a terminal hydroxamic acid group exhibited higher activity than Monastrol (38.2 ± 3.52 μM). Notably, derivatives **7f** and **7g**, obtained from 3-chlorobenzaldehyde and 4-chlorobenzaldehyde, respectively (Table 1, entries 16 and 17), demonstrated good potency, with IC_{50} values of 5.18 ± 0.89 μM and 6.70 ± 2.91 μM, respectively.

Among the ten compounds evaluated against MCF-7 cells, four derivatives bearing a terminal hydroxamic acid group displayed IC_{50} values below 1 μM (**7f–i**), while an additional four compounds exhibited IC_{50} values below 5 μM (**7a**, **7b**, **7e** and **7j**), identifying this series as particularly promising for breast cancer inhibition.

In particular, the hydroxamic acid derivative **7i** (Table 1, entry 19), synthesised from 4-methoxybenzaldehyde, showed an exceptionally low IC_{50} value of 0.02 ± 0.00 μM, representing the most potent compound within the DHPM–SAHA hybrid series. Furthermore, derivatives **7g**, **7h** and **7f**, derived from 4-chlorobenzaldehyde, 4-methylbenzaldehyde and 3-chlorobenzaldehyde, respectively (Table 1, entries 16–18), also exhibited significant antiproliferative activity, with IC_{50} values of 0.03 ± 0.01 μM, 0.04 ± 0.02 μM and 0.52 ± 0.20 μM, respectively.

The DHPM–SAHA hybrid **7j**, synthesised from furfuraldehyde, displayed submicromolar activity (IC_{50} = 1.21 ± 0.46 μM), indicating strong antiproliferative potency. Moreover, derivatives obtained from benzaldehyde, 2-chlorobenzaldehyde, and 2-hydroxybenzaldehyde (Table 1, entries 11, 15 and 12) also exhibited good activity, with IC_{50} values of 1.21 ± 0.46 μM, 3.32 ± 0.57 μM and 3.61 ± 0.40 μM, respectively.

Compared with our previously reported DHPM fatty acid derivatives, the DHPM–SAHA hybrids exhibited a marked enhancement in antiproliferative activity and a clear structure–

activity relationship.[24] While the earlier fatty acid derivatives showed moderate activity against AGS and MCF-7 cells (IC_{50} = 12.1–146.2 μM and 2.3–39.2 μM, respectively), only one derivative derived from 3-hydroxybenzaldehyde displayed an IC_{50} below 5 μM (2.3 ± 0.4 μM) against MCF-7 cells.

The introduction of a terminal hydroxamic acid moiety at the C5 side-chain of the DHPM core substantially improved potency against the breast cancer cell line MCF-7. Among the ten DHPM–SAHA hybrids evaluated, **7f–i** exhibited IC_{50} values below 1 μM, while **7a**, **7b**, **7e**, and **7j** showed IC_{50} values below 5 μM. These results highlight the crucial role of hydroxamic acid incorporation in enhancing antiproliferative activity.

This profile is consistent with previous reports by Huang and Pardee, who demonstrated that SAHA inhibited proliferation in the breast cancer cell lines MCF-7 and MDA-MB-231 in a dose-dependent manner at low micromolar concentrations (0.5–5 μM), with significant growth suppression observed at approximately 1–2.5 μM.[30] MCF-7 cells exhibited the highest sensitivity, confirming the potent antiproliferative effects associated with the hydroxamic acid pharmacophore.

Additionally, the calculated partition coefficient ($c\log P$) values of the most cytotoxic DHPM–SAHA hybrids were determined to estimate their lipophilicity. Compounds **7e–i** exhibited moderate lipophilicity, with $c\log P$ values ranging from 1.3 to 2.1, comparable to that of vorinostat ($c\log P = 1.9$).[31] Notably, derivatives bearing *para*-substituted phenyl groups—chloro (**7g**, $c\log P = 2.10$), methyl (**7h**, $c\log P = 1.89$), and methoxy (**7i**, $c\log P = 1.31$)—displayed remarkable potency (Fig. 5), with IC_{50} values below 0.05 μM, indicating strong antiproliferative activity.

These findings suggest that the enhanced cytotoxicity observed for these hybrids may be partially associated with their lipophilicity. According to the literature, lipophilicity plays a critical role in histone deacetylase (HDAC) inhibition by influencing both enzyme binding and intracellular activity.[32] Classical HDAC inhibitors, such as SAHA, follow a pharmacophoric model consisting of a zinc-binding group (typically a hydroxamic acid), a hydrophobic linker, and a surface-recognition (cap) group with an appropriate degree of lipophilicity. Because the HDAC catalytic site contains a predominantly hydrophobic channel leading to the Zn^{2+} ion, balanced lipophilicity enhances hydrophobic interactions within the active site and facilitates membrane permeability. However, this relationship is not strictly linear, as excessive lipophilicity may compromise aqueous solubility and pharmacokinetic properties. Therefore, optimal HDAC inhibition requires a well-balanced lipophilic profile that maximizes favorable enzyme interactions and cellular uptake while preserving drug-like characteristics.

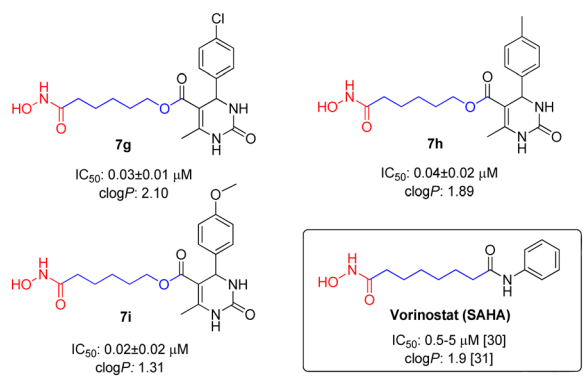

Fig. 5 Most cytotoxic DHPM–SAHA hybrids against the breast cancer cell line MCF-7.

Overall, the synthesized DHPM–SAHA hybrids, particularly compound **7i**, incorporate structural features characteristic of HDAC inhibitors, notably the presence of a zinc-binding hydroxamic acid capable of coordinating the catalytic Zn^{2+} ion within the enzyme active site. This modification establishes the classical HDAC pharmacophore architecture—comprising a zinc-binding group, a hydrophobic linker, and a surface-recognition cap group—positioning this hybrid scaffold as a promising platform for breast cancer therapy.

Conclusions

In summary, we synthesized a new series of 5-substituted dihydropyrimidinones (DHPMs) bearing a methoxy terminal group and their corresponding hydroxamic acid-containing DHPM–SAHA hybrids *via* the Biginelli multicomponent reaction, and evaluated their *in vitro* antitumor activity against AGS (gastric) and MCF-7 (breast) cancer cell lines.

All compounds exhibited low cytotoxicity toward SW872 human fibroblast cells (viability ≥ 70%). The derivatives showed greater activity against MCF-7 than AGS cells, with several compounds outperforming the reference drug Monastrol.

Among the ester derivatives, compound **6a** was the most active (IC_{50} = 1.33 ± 0.09 μM). Importantly, conversion of the terminal ester into hydroxamic acid–bearing DHPM–SAHA hybrids—incorporating a key zinc-binding motif characteristic of HDAC inhibitors such as Vorinostat—significantly enhanced antiproliferative activity.

The resulting hybrids displayed remarkable potency against both cell lines, with most compounds surpassing Monastrol. Compounds **7g**, **7h**, and **7f** exhibited submicromolar activity (IC_{50} = 0.03 ± 0.01, 0.04 ± 0.02, and 0.52 ± 0.20 μM, respectively), while **7i** was the most potent derivative of the series against MCF-7 cells (IC_{50} = 0.02 ± 0.00 μM).

Overall, hydroxamic acid incorporation and the multitarget DHPM–HDAC design strategy markedly improved anticancer activity. These findings highlight DHPM–SAHA hybrids as promising candidates for breast cancer therapy and warrant further mechanistic and *in vivo* investigations.

Experimental

General

All commercially available reagents were used without further purification. Sulfamic acid (98 wt%), urea, and thiourea were purchased from Sigma-Aldrich Chemical. The solvents employed in extraction and purification (hexane and ethyl acetate) were distilled before use. The reactions were monitored

by TLC (thin-layer chromatography) using pre-coated silica gel 60 F254 plates. The visualization was accomplished with UV light, stained with iodine. Flash chromatography was performed using Merck silica gel with a pore size of 60 Å, 230–400 mesh, with the indicated eluent system. The NMR spectra (^{1}H and ^{13}C) were obtained on a Bruker Nuclear Ascend 400 spectrometer. The spectra were obtained either in $CDCl_3$ or in DMSO-d_6 solution. The chemical shifts (δ) are reported in ppm and referenced to tetramethylsilane (TMS) as the internal standard. The coupling constants (J) are reported in hertz (Hz). Hydrogen coupling patterns are described as singlet (s), doublet (d), doublet of doublets (dd), doublet of doublet of doublets (ddd), doublet of triplets (dt), triplet (t), triplet of doublets (td), doublet of quartets (dq), quartet (q), quintet (quint), sextet (sext), broad signal (br), and multiplet (m). The melting points measured for some representative compounds were obtained on an MP90 melting point system.

Cell lines

A SW 872 (human fibroblast; HTB-92, ATCC) cell line was used, while AGS (gastric adenocarcinoma; CRL-1739, ATCC) and MCF-7 (mammary carcinoma; HTB-22, ATCC) were used as cancer cell lines. SW 872 and MCF7 cells were cultured in DMEM (Dulbecco's Modified Eagle Medium) medium (HyClone, Thermo Scientific USA); MCF-7′s medium was supplemented with human Insulin (10 μg mL^{-1}; Gibco, Thermo Scientific, USA) and AGS cells were cultured in RPMI-1640 medium (HyClone, Thermo Scientific), both medium were supplemented with 10% fetal bovine serum (FBS) (Hyclone™, GE Healthcare Life Science), 0.25 μg mL^{-1} amphotericin B (Hyclone™, GE Healthcare Life Science), and 25 μg mL^{-1} gentamicin (Millipore). Cells were maintained in an incubator at 37 °C, 5% CO_2.

Cell viability assay (MTT)

5.000 cells per well were seeded in a 96-well plate (SPL Life Sciences, Korea) for 12 hours, and each DHPM compounds were applied at 10 μM as treatment for 48 hours. The cells were washed with 100 μl of 1× PBS for 3 minutes, and then 100 μl of 0.5 mg mL^{-1} MTT/PBS 1× solution was added. The plate was then incubated for 90 minutes at 37 °C in an incubator. After discarding the MTT solution, 100 μl DMSO was loaded per well and kept stirring for 30 minutes. The plate was agitated for 30 min in darkness, and the absorbance was read at 570 nm using a spectrophotometer. For half maximal inhibitory concentration (IC_{50}) the same previous procedure was followed, but the following concentrations of all the compounds were measured; 1000 μM, 100 μM, 10 μM, 1 μM and 0.1 μM.

The MTT assays were conducted in triplicate. Data were saved in an Excel template (Microsoft®, Version 2108) and statistical analyses were performed in GraphPad Prism 8.0.1 (Graphpad Software, San Diego, CA).

Lipophilicity calculations

c log *P* values (logarithm of *n*-octanol/water partition coefficient *P*) were obtained by the software PerkinElmer ChemDraw®, Level: Professional, Version: 16.0.1.4 (77).

General procedure for the synthesis of hydroxyester 3

In a round-bottom flask, ε-caprolactone **2** (1 equivalent), sulfamic acid (NH_2SO_3H, 30 mol%) and methanol (proportion of 10 mL for 1 mmol of starting material) were added. The reaction was kept under stirring and reflux for 4 hours. After completion of the reaction, the catalyst was filtered and the solvent removed under reduced pressure. Compound **5** was obtained quantitatively and used in the subsequent step without the need of purification.

General procedure for the synthesis of β-ketoester 5

In a round bottom flask, methyl 6-hydroxyhexanoate **3** (1 equivalent), TMD **4** (2,2,6-Trimethyl-4*H*-1,3-dioxin-4-one, 1.3 equivalent) were added, anhydrous sodium NaOAc (1 equivalent) and THF as solvent. The reaction mixture was kept under stirring for 24 hours at 100 °C. Then, a liquid–liquid extraction was carried out with diethyl ether and saturated sodium chloride solution. The collected organic phase was dried with $MgSO_4$, filtered and the solvent removed *via* rotary evaporation.

General procedure for synthesis of 5-substituited DHPM 6a–j

In a round-bottom flask, the aromatic aldehyde (1 equivalent), β-ketoester **3** (1 equivalent), urea (1 equivalent) and the catalyst sulfamic acid (NH_2SO_3H, 20 mol%) in methanol (MeOH) as solvent. The mixture was kept under reflux and constant stirring for 24 hours. After completion of the reaction, the reaction crude was subjected to purification by column chromatography or recrystallization.

General procedure for synthesis of DHPM–SAHA molecular hybrids 7a–j

In a round-bottom flask A, hydroxylamine hydrochloride (18.4 mmol) in methanol was added, kept under stirring at 40 °C. A solution of KOH (18.4 mmol) in methanol was slowly added to the flask containing hydroxylamine hydrochloride to release the hydroxylamine into the reaction medium. After 0.5 hours, the mixture was cooled to 0 °C and filtered (to remove the formed potassium chloride) directly into another flask containing the precursor **6a–j** (1 mmol) and methanol (2 mL), previously heated at 85 °C for dissolution. After completion of filtration and addition of the released hydroxylamine, the heating bath was removed so the reaction could occur at room temperature. Subsequently, 0.094 g of KOH was slowly added to reach alkaline pH (pH above 10). The reaction remained under agitation overnight. Afterwards, the mixture was added to 32 mL of water at 0 °C under stirring and the pH was adjusted to 7 with the addition of acetic acid. The precipitate **7a–j** formed was filtered under vacuum.

6-Methoxy-6-oxohexyl 6-methyl-2-oxo-4-phenyl-1,2,3,4-tetrahydro-pyrimidine-5-carboxylate (6a). MW = 360.41 g mol^{-1}; white solid; M. P. 128–131 °C; yield: 55%; ^{1}H NMR (400 MHz, DMSO-d_6): δ (ppm) 9.19 (s, 1H), 7.72 (s, 1H), 7.34–7.22 (m, 5H), 5.13 (d, 1H, ^3J = 3.2 Hz), 3.98–3.86 (m, 2H), 3.57 (s, 3H), 2.26 (s, 3H), 2.21 (t, 3H, ^3J = 7.4 Hz), 1.47–1.40 (m, 4H), 1.13–1.09 (m, 2H); ^{13}C NMR (100 MHz, DMSO-d_6): 173.7, 165.8, 152.5,

149.1, 145.2, 128.8, 127.7, 126.7, 99.4, 63.4, 54.5, 51.6, 33.5, 28.3, 25.4, 24.4, 18.2; IR (max, cm^{-1}): 3231; 3120; 2956; 1736; 1699; 1650; 1433; 1289; 1221; 1094; 806.

6-Methoxy-6-oxohexyl 4-(2-hydroxyphenyl)-6-methyl-2-oxo-1,2,3,4 tetrahydropyrimidine-5-carboxylate (6b). MW = 376.41 g mol^{-1}; white solid; M. P. 133–136 °C; yield: 30%; ^{1}H NMR (400 MHz, DMSO-d_6): δ (ppm) 9.57 (s, 1H), 9.09 (s, 1H), 7.06–7.02 (m, 2H), 6.95 (dd, 1H, ^3J = 7.6 Hz, ^3J = 1.4 Hz), 6.80–6.78 (m, 1H), 6.72–6.69 (m, 1H), 5.47 (d, 1H, ^3J = 2.8 Hz), 3.94–3.88 (m, 1H), 3.86–3.80 (m, 1H), 3.57 (s, 3H), 2.28 (s, 3H), 2.18 (t, 3H, ^3J = 7.5 Hz), 1.42–1.35 (m, 4H), 1.09–1.01 (m, 2H); ^{13}C NMR (100 MHz, DMSO-d_6): 173.7, 165.9, 155.1, 152.7, 149.3, 130.3, 128.7, 127.5, 119.2, 115.8, 98.1, 63.2, 51.6, 49.4, 33.6, 28.3, 25.3, 24.5, 18.1; IR (max, cm^{-1}): 3422; 3229; 3098; 2948; 1732; 1679; 1656; 1455; 1260; 1235; 1084; 757.

6-Methoxy-6-oxohexyl 4-(3-hydroxyphenyl)-6-methyl-2-oxo-1,2,3,4-tetrahydropyrimidine-5-carboxylate (6c). MW = 376.41 g mol^{-1}; white solid; M. P. 128–130 °C; yield: 55%; ^{1}H NMR (400 MHz, DMSO-d_6): δ (ppm) 9.34 (s, 1H), 9.15 (s, 1H), 7.66 (s, 1H), 7.11–7.07 (m, 1H), 6.66–6.61 (m, 3H), 5.04 (d, 1H, ^3J = 3.3 Hz), 3.98–3.89 (m, 2H), 3.57 (s, 3H), 2.25–2.21 (m, 5H), 1.49–1.43 (m, 4H), 1.16–1.12 (m, 2H); ^{13}C NMR (100 MHz, DMSO-d_6): 173.7, 165.9, 157.8, 152.5, 148.8, 146.6, 129.7, 117.4, 114.6, 113.5, 99.6, 63.4, 54.4, 51.6, 33.6, 28.3, 25.4, 24.5, 18.2; IR (max, cm^{-1}): 3364; 3229; 3106; 2946; 1704; 1646; 1591; 1459; 1293; 1223; 1088; 790.

6-Methoxy-6-oxohexyl 4-(4-hydroxyphenyl)-6-methyl-2-oxo-1,2,3,4-tetrahydropyrimidine-5-carboxylate (6d). MW = 376.41 g mol^{-1}; white solid; M. P. 139–142 °C; yield: 60%; ^{1}H NMR (400 MHz, DMSO-d_6): δ (ppm) 9.32 (s, 1H), 9.10 (s, 1H), 7.59 (s, 1H), 7.01 (d, 2H, ^3J = 8.5 Hz), 6.68 (d, 2H, ^3J = 8.4 Hz), 5.02 (d, 1H, ^3J = 3.1 Hz), 3.99–3.85 (m, 2H), 3.58 (s, 3H), 2.24–2.21 (m, 5H), 1.49–1.41 (m, 4H), 1.17–1.12 (m, 2H); ^{13}C NMR (100 MHz, DMSO-d_6): 173.7, 165.9, 157.0, 152.5, 148.5, 135.8, 127.9, 115.4, 99.9, 63.4, 53.9, 51.6, 33.6, 28.3, 25.4, 24.5, 18.2; IR (max, cm^{-1}): 3249; 3118; 2952; 1685; 1644; 1457; 1318; 1229; 1077; 757.

6-Methoxy-6-oxohexyl 4-(2-chlorophenyl)-6-methyl-2-oxo-1,2,3,4-te-trahydropyrimidine-5-carboxylate (6e). MW = 394.85 g mol^{-1}; white solid; M. P. 137–140 °C; yield: 52%; ^{1}H NMR (400 MHz, DMSO-d_6): δ (ppm) 9.28 (s, 1H), 7.68 (s, 1H), 7.41–7.39 (m, 2H), 7.32–7.27 (m, 3H), 5.62 (d, 1H, ^3J = 3.0 Hz), 3.92–3.86 (m, 1H), 3.84–3.80 (m, 1H), 3.57 (s, 3H), 2.31 (s, 3H), 2.18 (t, 3H, ^3J = 7.4 Hz), 1.41–1.34 (m, 4H), 1.03–0.94 (m, 2H); ^{13}C NMR (100 MHz, DMSO-d_6): 173.6, 165.4, 151.8, 150.2, 142.1, 132.2, 129.9, 129.8, 129.6, 129.5, 129.1, 129.0, 128.2, 98.1, 63.3, 51.9, 51.8, 51.6, 51.2, 33.6, 28.2, 25.3, 24.5, 18.1; IR (max, cm^{-1}): 3344; 3219; 3104; 2950; 1728; 1695; 1644; 1461; 1225; 1098; 763.

6-Methoxy-6-oxohexyl 4-(3-chlorophenyl)-6-methyl-2-oxo-1,2,3,4-te-trahydropyrimidine-5-carboxylate (6f). MW = 394.85 g mol^{-1}; white solid; M. P. 132–134 °C; yield: 55%; ^{1}H NMR (400 MHz, DMSO-d_6): δ (ppm) 9.26 (s, 1H), 7.77 (s, 1H), 7.39–7.30 (m, 2H), 7.24–7.18 (m, 3H), 5.16–5.14 (m, 1H), 4.01–3.95 (m, 1H), 3.91–3.85 (m, 1H), 3.57 (s, 3H), 2.27 (s, 3H), 2.23 (t, 3H, ^3J = 7.4 Hz), 1.47–1.39 (m, 4H), 1.14–1.07 (m, 2H); ^{13}C NMR (100 MHz, DMSO-d_6): 173.7, 165.6, 152.3, 149.7, 147.6, 131.0, 127.7, 126.7, 125.4, 128.2, 98.8, 63.5, 54.1, 33.6, 28.3, 25.4, 24.5, 18.3; IR (max, cm^{-1}): 3307; 3237; 3108; 2946; 1704; 1654; 1437; 1242; 1090; 767.

6-Methoxy-6-oxohexyl 4-(4-chlorophenyl)-6-methyl-2-oxo-1,2,3,4-te-trahydropyrimidine-5-carboxylate (6g). MW = 394.85 g mol^{-1}; white solid; M. P. 123–125 °C; yield: 60%; ^{1}H NMR (400 MHz, DMSO-d_6): δ (ppm) 9.24 (s, 1H), 7.76–7.75 (m, 1H), 7.39 (d, 2H, ^3J = 8.5 Hz), 7.24 (d, 2H, ^3J = 8.4 Hz), 5.13 (d, 1H, ^3J = 3.2 Hz), 3.99–3.85 (m, 2H), 3.58 (s, 3H), 2.27–2.20 (m, 5H), 1.47–1.39 (m, 4H), 1.13–1.07 (m, 2H); ^{13}C NMR (100 MHz, DMSO-d_6): 173.7, 165.6, 152.2, 149.5, 144.1, 132.3, 128.8, 128.6, 99.0, 63.4, 51.6, 33.5, 28.3, 25.4, 24.4, 18.2; IR (max, cm^{-1}): 3330; 3223; 3095; 2948; 1724; 1695; 1646; 1465; 1227; 1088; 823.

6-Methoxy-6-oxohexyl 6-methyl-2-oxo-4-(*p*-tolyl)-1,2,3,4-tetrahy-dropyrimidine-5-carboxylate (6h). MW = 374.44 g mol^{-1}; white solid; M. P. 136–139 °C; yield: 50%; ^{1}H NMR (400 MHz, DMSO-d_6): δ (ppm) 9.15 (s, 1H), 7.66 (s, 1H), 7.11 (s, 4H), 5.09 (d, 1H, ^3J = 3.2 Hz), 3.98–3.85 (m, 2H), 3.58 (s, 3H), 2.26–2.18 (m, 8H), 1.48–1.39 (m, 4H), 1.14–1.06 (m, 2H); ^{13}C NMR (100 MHz, DMSO-d_6): 173.7, 165.8, 152.5, 148.9, 142.3, 136.9, 129.4, 126.6, 99.6, 63.4, 54.2, 51.6, 33.6, 28.3, 25.4, 24.5, 21.1, 18.2; IR (max, cm^{-1}): 3241; 3114; 2950; 1724; 1706; 1652; 1465; 1433; 1285; 1227; 1090; 788.

6-Methoxy-6-oxohexyl 4-(4-methoxyphenyl)-6-methyl-2-oxo-1,2,3,4-tetrahydropyrimidine-5-carboxylate (6i). MW = 390.44 g mol^{-1}; white solid; M. P. 102–104 °C; yield: 70%; ^{1}H NMR (400 MHz, DMSO-d_6): δ (ppm) 9.19 (s, 1H), 7.72 (s, 1H), 7.32–7.30 (m, 2H), 7.25–7.22 (m, 2H), 5.13 (d, 1H, ^3J = 2.9 Hz), 3.98–3.87 (m, 2H), 3.57 (s, 3H), 2.26 (s, 3H), 2.21 (t, 2H, ^3J = 7.4 Hz), 1.47–1.41 (m, 4H), 1.15–1.09 (m, 2H); ^{13}C NMR (100 MHz, DMSO-d_6): 173.7, 165.8, 152.5, 149.1, 145.2, 128.8, 127.7, 126.7, 99.4, 63.4, 54.5, 51.6, 33.6, 28.3, 25.4, 24.4, 18.2; IR (max, cm^{-1}): 3241; 3110; 2952; 1730; 1701; 1648; 1437; 1221; 1096; 1030; 788.

6-Methoxy-6-oxohexyl 4-(furan-2-yl)-6-methyl-2-oxo-1,2,3,4-tetra-hydropyrimidine-5-carboxylate (6j). MW = 350.37 g mol^{-1}; white solid; M. P. 138–140 °C; yield: 45%; ^{1}H NMR (400 MHz, DMSO-d_6): δ (ppm) 9.23 (s, 1H), 7.75–7.75 (m, 1H), 7.54 (s, 1H), 6.36–6.35 (m, 1H), 6.09 (m, 1H), 5.20 (d, 1H, ^3J = 3.3 Hz), 4.04–3.91 (m, 2H), 3.58 (s, 3H), 2.28–2.24 (m, 5H), 1.53–1.45 (m, 4H), 1.23–1.18 (m, 2H); ^{13}C NMR (100 MHz, DMSO-d_6): 173.2 (2C),165.0, 155.8, 152.3, 149.4, 142.0, 110.2, 105.2, 96.6, 62.9, 51.1, 47.6, 33.0, 27.7, 24.8, 23.9, 17.6; IR (max, cm^{-1}): 3239; 3114; 2956; 1734; 1701; 1652; 1435; 1223; 1084; 800.

6-(hydroxyamino)-6-oxohexyl 6-methyl-2-oxo-4-phenyl-1,2,3,4-te-trahydropyrimidine-5-carboxylate (8a). MW = 361.40 g mol^{-1}; white solid; M. P. 98–100 °C; yield: 50%; ^{1}H NMR (400 MHz, DMSO-d_6): δ (ppm) 10.33 (s, 1H), 9.19 (s, 1H), 8.67 (s, 1H), 7.72 (s, 1H), 7.34–7.31 (m, 2H), 7.26–7.22 (m, 3H), 5.13 (d, 1H, ^{3}J = 3.1 Hz), 3.96–3.86 (m, 2H), 2.26 (s, 3H), 1.88 (t, 2H, ^{3}J = 7.4 Hz), 1.47–1.37 (m, 4H), 1.15–1.09 (m, 2H); ^{13}C NMR (100 MHz, DMSO-d_6): d (ppm) 169.4, 165.8, 152.5, 149.0, 145.2, 128.9, 127.7, 126.7, 99.5, 63.5, 54.5, 32.5, 28.3, 25.5, 25.2, 18.2; IR (max, cm-1): 3235; 2937; 1726; 1693; 1648; 1229; 759.

6-(hydroxyamino)-6-oxohexyl 4-(2-hydroxyphenyl)-6-methyl-2-oxo-1,2,3,4-tetrahydropyrimidine-5-carboxylate (8b). MW = 377.41 g mol^{-1}; white solid. M. P. 149–151 °C; yield: 66%; ^{1}H NMR (400 MHz, DMSO-d_6): δ (ppm) 9.09 (s, 1H), 7.72 (s, 1H), 7.06–7.03 (m, 2H), 6.95 (dd, 1H, ^3J = 7.6 Hz, ^3J = 1.4 Hz), 6.81–6.79 (m, 1H), 6.73–6.69 (m, 1H), 5.47 (s, 1H), 3.93–3.81 (m, 2H),

2.28 (s, 3H), 1.85 (t, 2H, ^3J = 7.4 Hz), 1.42–1.33 (m, 4H), 1.09–1.04 (m, 2H); ^{13}C NMR (100 MHz, DMSO-d_6): δ (ppm) 169.5, 165.9, 155.1, 152.7, 149.3, 130.3, 128.7, 127.5, 119.2, 115.9, 98.2, 63.3, 49.4, 32.5, 28.3, 25.4, 25.2, 18.2; IR (max, cm^{-1}): 3379; 3266; 2954; 1689; 1648; 1463; 1229; 1102; 759.

6-(hydroxyamino)-6-oxohexyl 4-(3-hydroxyphenyl)-6-methyl-2-oxo-1,2,3,4-tetrahydropyrimidine-5-carboxylate (8c). MW = 377.41 g mol^{-1}; white solid. M. P. 147–149 °C; yield: 48%; ^{1}H NMR (400 MHz, DMSO-d_6): δ (ppm) 10.33 (s, 1H), 9.37 (s, 1H), 9.14 (s, 1H), 8.67 (s, 1H), 7.65 (s, 1H), 7.11–7.07 (m, 1H), 6.67–6.60 (m, 3H), 5.04 (d, 1H, ^3J = 3.2 Hz), 3.98–3.87 (m, 2H), 2.24 (s, 3H), 1.89 (t, 2H, ^3J = 7.3 Hz), 1.49–1.41 (m, 4H), 1.18–1.13 (m, 2H); ^{13}C NMR (100 MHz, DMSO-d_6): δ (ppm) 169.5, 165.9, 157.8, 152.6, 148.7, 146.6, 129.8, 117.4, 114.7, 113.5, 99.7, 63.6, 54.3, 32.6, 28.3, 25.5, 25.2, 18.3; IR (max, cm^{-1}): 3230; 3108; 2940; 2850; 1670; 1459; 1232; 1080; 779.

6-(hydroxyamino)-6-oxohexyl 4-(4-hydroxyphenyl)-6-methyl-2-oxo-1,2,3,4-tetrahydropyrimidine-5-carboxylate (8d). MW = 377.41 g mol^{-1}; white solid; M. P. 145–147 °C; yield: 52%; ^{1}H NMR (400 MHz, DMSO-d_6): δ (ppm) 9.10 (s, 1H), 7.60 (s, 1H), 7.03–7.00 (m, 2H), 6.70–6.68 (m, 1H), 5.03 (d, 1H, ^3J = 3.0 Hz), 3.96–3.86 (m, 2H), 2.24 (s, 3H), 1.90 (t, 2H, ^3J = 7.3 Hz), 1.48–1.41 (m, 4H), 1.16–1.10 (m, 2H); ^{13}C NMR (100 MHz, DMSO-d_6): δ (ppm) 169.4, 165.9, 157.0, 152.5, 148.4, 135.8, 127.8, 115.5, 100.0, 63.5, 53.9, 32.5, 28.3, 25.5, 25.2, 18.2; IR (max, cm^{-1}): 3348; 3252; 3106; 2937; 1710; 1636; 1453; 1221; 1102; 800.

6-(hydroxyamino)-6-oxohexyl 4-(2-chlorophenyl)-6-methyl-2-oxo-1,2,3,4-tetrahydropyrimidine-5-carboxylate (8e). MW = 395.84 g mol^{-1}; white solid; M. P. 119–122 °C; yield: 50%; ^{1}H NMR (400 MHz, DMSO-d_6): δ (ppm) 10.31 (s, 1H), 9.27 (s, 1H), 8.65 (s, 1H), 7.68 (s, 1H), 7.42–7.40 (m, 1H), 7.32–7.26 (m, 3H), 5.62 (d, 1H, ^3J = 2.9 Hz), 3.89–3.78 (m, 2H), 2.31 (s, 3H), 1.83 (t, 2H, ^3J = 7.5 Hz), 1.40–1.31 (m, 4H), 1.01–0.95 (m, 2H); ^{13}C NMR (100 MHz, DMSO-d_6): δ (ppm) 1689, 164.9, 151.2, 149.5, 141.5, 131.6, 129.3, 129.0, 128.5, 127.7, 97.6, 62.9, 51.3, 32.0, 27.7, 24.8, 24.6, 17.6; IR (max, cm^{-1}): 3230; 3109; 2940; 2846; 1700; 1648; 1227; 1089; 815.

6-(hydroxyamino)-6-oxohexyl 4-(3-chlorophenyl)-6-methyl-2-oxo-1,2,3,4-tetrahydropyrimidine-5-carboxylate (8f). MW = 395.84 g mol^{-1}; white solid; M. P. 105–107 °C; yield: 50%; ^{1}H NMR (400 MHz, DMSO-d_6): δ (ppm) 9.27 (d, 1H, ^3J = 5.6 Hz), 7.78 (dd, 1H, ^3J = 12 Hz, ^3J = 3.0 Hz), 7.37–7.32 (m, 2H), 7.24–7.18 (m, 2H), 5.16–5.14 (m, 1H), 3.98–3.87 (m, 1H), 2.26 (s, 3H), 1.88 (t, 2H, ^3J = 7.3 Hz), 1.47–1.37 (m, 4H), 1.14–1.09 (m, 2H); ^{13}C RMN (100 MHz, DMSO-d_6): δ (ppm) 169.4, 166.2, 165.7, 152.4, 149.7, 133.4, 131.0, 127.8, 126.6, 125.3, 98.9, 63.7, 53.9, 51.4, 32.5, 28.3, 25.5, 25.2, 18.3; IR (max, cm^{-1}): 3348; 3305; 2946; 1673; 1658; 1437; 1240; 1094; 759.

6-(Hydroxyamino)-6-oxohexyl 4-(4-chlorophenyl)-6-methyl-2-oxo-1,2,3,4-tetrahydropyrimidine-5-carboxylate (8g). MW = 395.84 g mol^{-1}; white solid; M. P. 100–103 °C; yield: 51%; ^{1}H NMR (400 MHz, DMSO-d_6): δ (ppm) 9.23 (s, 1H), 7.74 (d, 1H, ^3J = 2.4 Hz), 7.40–7.38 (m, 2H), 7.24–7.22 (m, 2H), 5.13 (d, 1H, ^3J = 3.2 Hz), 3.97–3.86 (m, 2H), 2.25 (s, 3H), 1.88 (t, 2H, ^3J = 7.6 Hz), 1.46–1.39 (m, 4H), 1.12–1.09 (m, 2H); ^{13}C NMR (100 MHz, DMSO-d_6): δ (ppm) 169.5, 165.7, 152.3, 149.4, 144.2, 132.3, 128.9, 128.7, 100.6, 64.1, 53.9, 36.1, 28.4, 25.8, 25.4, 17.6; IR (max, cm^{-1}): 3241; 3126; 2950; 1697; 1644; 1461; 1229; 1090; 769.

6-(Hydroxyamino)-6-oxohexyl 6-methyl-2-oxo-4-(*p*-tolyl)-1,2,3,4-tetrahydropyrimidine-5-carboxylate (8h). MW = 375.43 g mol^{-1}; white solid; M. P. 111–113 °C; yield: 60%; ^{1}H NMR (400 MHz, DMSO-d_6): δ (ppm) 9.14 (s, 1H), 7.65 (d, 2H, ^3J = 2.6 Hz), 7.11 (s, 4H), 5.09 (d, 1H, ^3J = 3.0 Hz), 3.96–3.87 (m, 2H), 2.25 (s, 3H), 2.24 (s, 3H), 1.87 (t, 2H, ^3J = 7.3 Hz), 1.48–1.37 (m, 4H), 1.15–1.10 (m, 2H); ^{13}C NMR (100 MHz, DMSO-d_6): δ (ppm) 169.4, 165.9, 152.6, 148.8, 142.3, 136.9, 129.4, 126.6, 99.7, 63.5, 542, 32.6, 28.4, 25.5, 25.2, 21.1, 18.2; IR (max, cm^{-1}): 3256; 3108; 2948; 1699; 1652; 1465; 1229; 1096; 776.

6-(Hydroxyamino)-6-oxohexyl 4-(4-methoxyphenyl)-6-methyl-2-oxo-1,2,3,4-tetrahydropyrimidine-5-carboxylate (8i). MW = 391.42 g mol^{-1}; white solid; M. P. 118–121 °C; yield: 42%; ^{1}H NMR (400 MHz, DMSO-d_6): δ (ppm) 10.32 (s, 1H), 9.14 (s, 1H), 8.66 (s, 1H), 7.64 (s, 1H), 7.14–7.12 (m, 2H), 6.89–6.97 (m, 2H), 5.08 (d, 1H, ^3J = 3.0 Hz), 3.95–3.86 (m, 2H), 3.72 (s, 3H), 2.25 (s, 3H), 1.89 (t, 2H, ^3J = 7.4 Hz), 1.48–1.38 (m, 4H), 1.17–1.11 (m, 2H); ^{13}C NMR (100 MHz, DMSO-d_6): δ (ppm) 169.4, 165.9, 157.0, 152.5, 148.4, 135.8, 127.8, 115.5, 100.0, 63.5, 53.9, 32.5, 28.3, 25.5, 25.2, 18.2; IR (max, cm^{-1}): 3358; 3221; 3130; 2946; 1706; 1644; 1513; 1453; 1233; 1098; 833.

6-(Hydroxyamino)-6-oxohexyl 4-(furan-2-yl)-6-methyl-2-oxo-1,2,3,4-tetrahydropyrimidine-5-carboxylate (8j). MW = 351.36 g mol^{-1}; white solid; M. P. 157–160 °C; yield: 49%; ^{1}H NMR (400 MHz, DMSO-d_6): δ (ppm) 10.38 (s, 1H), 9.29 (s, 1H), 8.71 (s, 1H), 7.79 (s, 1H), 7.60 (s, 1H), 6.42–6.41 (m, 1H), 6.14 (d, 1H, ^3J = 3.0 Hz), 5.25 (d, 1H, ^3J = 3.2 Hz), 4.08–3.96 (m, 2H), 2.29 (s, 3H), 1.96 (t, 2H, ^3J = 7.3 Hz), 1.57–1.47 (m, 4H), 1.28–1.20 (m, 2H); ^{13}C NMR (100 MHz, DMSO-d_6): δ (ppm) 168.9, 164.9, 155.9, 152.3, 149.4, 142.0, 110.3, 105.2, 96.6, 63.0, 47.6, 32.0, 27.8, 25.0, 24.6, 17.6; IR (max, cm^{-1}): 3381; 3239; 3118; 2950; 1730; 1691; 1642; 1463; 1240; 1112; 788.

Author contributions

Conceptualization: M. G. M. D'Oca and C. D. R Montes D'Oca synthesis and characterization of molecules: E. A. M. Rios, C. M. Dea, E. R. F. B. dos Santos and G. M. S. D. M. Pereira experiment for identification: E. A. M. Rios and G. M. S. D. M. Pereira biological assays: L. S. Santos, F. M. Nachtigall, L. Guzman, R. Moore-Carrasco, D. Rebolledo-Miraf resources: M. G. M. D'Oca, D. S. Rampon and C. D. R Montes D'Oca data curation: E. A. M. Rios and G. M. S. D. M. Pereira writing – original draft: E. A. M. Rios and C. D. R Montes D'Oca writing – review & editing: M. G. M. D'Oca, C. D. R Montes D'Oca, D. S. Rampon and L. S. Santos project administration: Marcelo G. M. D'Oca and Caroline D. R Montes D'Oca funding acquisition: Marcelo G. M. D'Oca, D. S. Rampon, Caroline D. R Montes D'Oca and L. S. Santos.

Conflicts of interest

The authors declare no competing interests.

Data availability

The data supporting this article have been included as part of the supplementary information (SI). Supplementary

information: ^{1}H, ^{13}C NMR spectra and Infrared spectra. See DOI: https://doi.org/10.1039/d6ra00701e.

Acknowledgements

The authors are thankful for financial support from Coordenação de Aperfeiçoamento de Pessoal de Nivel Superior (CAPES), and Conselho Nacional de Desenvolvimento Científico e Tecnológico (CNPq). Fellowships from CAPES are also acknowledged.

References

1 O. M. Soltan, M. E. Shoman, S. A. Abdel-Aziz, A. Narumi, H. Konno and M. Abdel-Aziz, *Eur. J. Med. Chem.*, 2021, **225**, 113768.
2 K. Nepali, S. Sharma, M. Sharma, P. M. S. Bedi and K. L. Dhar, *Eur. J. Med. Chem.*, 2014, **77**, 422–487.
3 K. Bukowski, M. Kciuk and R. Kontek, *Int. J. Mol. Sci.*, 2020, **21**, 3233.
4 E. Marchesi, D. Perrone and M. L. Navacchia, *Pharmaceutics*, 2023, **15**, 2185.
5 Shalini and V. Kumar, *Expert Opin. Drug Discov.*, 2021, **16**, 335–363.
6 A. K. Singh, A. Kumar, H. Singh, P. Sonawane, H. Paliwal, S. Thareja, P. Pathak, M. Grishina, M. Jaremko and A.-H. Emwas, *Pharmaceuticals*, 2022, **15**, 1071.
7 L. H. S. Matos, F. T. Masson, L. A. Simeoni and M. H. de Mello, *Eur. J. Med. Chem.*, 2018, **143**, 1779–1789.
8 P. Biginelli, *Ber. Dtsch. Chem. Ges.*, 1891, **24**, 1317–1319.
9 H. Nagarajaiah, A. Mukhopadhyay and J. N. Moorthy, *Tetrahedron Lett.*, 2016, **57**, 5135–5149.
10 S. R. Patil, A. S. Choudhary, V. S. Patil and N. Sekar, *Fibers Polym.*, 2015, **16**, 2349–2356.
11 A. Fauzi, A. Saifudin and K. Rullah, *J. Med. Chem. Sci.*, 2023, **6**, 1810–1821.
12 Z. Maliga, T. M. Kapoor and T. J. Mitchison, *Chem. Biol.*, 2002, **9**, 989–996.
13 U. Mayer, T. M. Kapoor, S. J. Haggarty, R. W. King, S. L. Schreiber and T. J. Mitchison, *Science*, 1999, **286**, 971.
14 S. Grant, C. Easley and P. Kirkpatrick, *Nat. Rev. Drug Discovery*, 2007, **6**, 21–22.
15 S. Geurs, D. Clarisse, K. De Bosscher and M. D'hooghe, *J. Med. Chem.*, 2023, **66**, 7698–7715.
16 A. Wawruszak, L. Borkiewicz, E. Okon, W. Kukula-Koch, S. Afshan and M. Halasa, *Cancers*, 2021, **13**, 4700.
17 B. S. Mann, J. R. Johnson, M. H. Cohen, R. Justice and R. Pazdur, *Oncologist*, 2007, **12**, 1247–1252.
18 N. Q. Khai and T. K. Vu, *Anti-Cancer Agents Med. Chem.*, 2024, **24**, 18–35.
19 N. Zhao, F. Yang, L. Han, Y. Qu, D. Ge and H. Zhang, *Molecules*, 2020, **25**, 717.
20 S. García, I. Mercado-Sánchez, L. Bahena, Y. Alcaraz, M. A. García-Revilla, J. Robles, N. Santos-Martínez, D. Ordaz-Rosado, R. García-Becerra and M. A. Vázquez, *Molecules*, 2020, **25**, 5134.
21 J. Yan, K. Yue, X. Fan, X. Xu, J. Wang, M. Qin, Q. Zhang, X. Hou, X. Li and Y. Wang, *Eur. J. Med. Chem.*, 2023, **246**, 115004.
22 D. A. Preciado, A. F. Yepes, A. Herrera and W. Cardona, *Med. Chem. Res.*, 2024, **33**, 1511–1524.
23 Z. Lv, T. Ji, J. Liu, X. Sun and H. Liang, *Eur. J. Med. Chem.*, 2025, **283**, 117185.
24 E. A. M. Rios, C. M. Dea, E. R. B. dos Santos, M. G. Montes D'Oca, D. S. Rampon, F. M. Nachtigall, L. S. Santos, L. Guzman, R. Moore-Carrasco, D. Rebolledo-Miraf and C. D. R. Montes D'Oca, *RSC Adv.*, 2024, **14**, 22981–22992.
25 V. Vendrusculo, V. P. de Souza, L. A. M. Fontoura, M. G. M. D'Oca, T. P. Banzato, P. A. Monteiro, R. A. Pilli, J. E. de Carvalho and D. Russowsky, *Med. Chem. Commun.*, 2018, **9**, 1553–1564.
26 F. S. De Oliveira, P. M. De Oliveira, L. M. Farias, R. C. Brinkerhoff, R. C. M. A. Sobrinho, T. M. Treptow, C. R. Montes D'Oca, M. A. G. Marinho, M. A. Hort, A. P. Horn, D. Russowsky and M. G. Montes D'Oca, *Med. Chem. Commun.*, 2018, **9**, 1282–1288.
27 T. G. M. Treptow, F. Figueiró, E. H. F. Jandrey, A. M. O. Battastini, C. G. Salbego, J. B. Hoppe, P. S. Taborda, S. B. Rosa, L. A. Piovesan, C. D. R. Montes D'Oca, D. Russowsky and M. G. Montes D'Oca, *Eur. J. Med. Chem.*, 2015, **95**, 552–562.
28 M. G. Montes D'Oca, R. M. Soares, R. R. de Moura and V. F. Granjão, *Fuel*, 2012, **97**, 884–886.
29 A. Samiei, M. A. Bodaghifard and M. Hamidinasab, *Curr. Green Chem.*, 2024, **11**, 194–203.
30 L. Huang and A. B. Pardee, *Mol. Med.*, 2000, **6**, 849–866.
31 National Center for Biotechnology Information (NCBI), *PubChem Compound Summary for CID 5311*, Vorinostat, 2026, https://pubchem.ncbi.nlm.nih.gov/compound/5311 accessed February 2026.
32 P. A. Marks, V. M. Richon and R. A. Rifkind, *Nat. Rev. Cancer*, 2001, **1**, 194–202.